Characterization of low frequency instabilities and study of their transition to turbulence in a magnetized plasma column

F. Brochard, Gildas Bonhomme, E. Gravier

Characterization of low frequency instabilities and study of their transition to turbulence in a magnetized plasma column

F. Brochard, G. Bonhomme, E. Gravier

LPMIA UMR 7040 CNRS, Université Henri Poincaré – Nancy 1
Boulevard des Aiguillettes BP 239 – 54506 VANDOEUVRE-Lès-NANCY cedex FRANCE

ABSTRACT

In this contribution we report on experiments performed on the low-β plasma device MIRABELLE. Using a limiter, we recently got experimental evidence that when increasing the magnetic field transitions between various gradient driven instabilities are observed. The characterization is based on: (i) comparison between the poloidal propagation velocity and the diamagnetic and E×B velocities deduced from measurements of the density and plasma potential profiles; (ii) measurements of the axial wave number. Moreover, these results are corroborated by measurements of the radial variation of the phase of the fluctuations. More precisely, at low magnetic field the strong $E_r \times B$ velocity shear drives a Kelvin-Helmholtz instability, whereas at higher magnetic field drift waves are only observed [1]. In between we also observed in some cases a centrifugal (Rayleigh-Taylor) instability.

With regards to the role played by these instabilities in non-diffusive transport processes in plasma fusion experiments, and aiming at characterizing the turbulent transport, we studied the transition from regular regimes to spatiotemporal chaos and turbulence. We demonstrate that for the Kelvin-Helmholtz instability the transition to turbulence follows the quasi-periodicity (Ruelle-Takens-Newhouse) route, as previously observed for drift waves [2]. Moreover, temporal analysis of the quasi-periodic regime gives clear evidences of an autonomous periodic pulling regime, i.e. incomplete entrainment. Recent results about the transition to turbulence for a Rayleigh-Taylor instability will also be presented.

1. INTRODUCTION

Since early observations [3], low frequency instabilities in bounded magnetized plasmas have attracted much attention because of their role in enhanced non diffusive transport across the magnetic field [4]. Though low frequency plasma density fluctuations are easily observed in linear magnetized plasma columns, it is not not so easy to clearly determine to which class of instability these fluctuations belong. In this work, we demonstrate that using a limiter, it becomes possible to observe three low frequency instabilities, similar to those which developp in the edge of a fusion experiment. This contribution is organized as follows. We first give in section 2 a brief theoretical overview of the three instabilities met in our study : the drift waves, centrifugal, and Kelvin-Helmholtz instabilities. In section 3, we introduce our experimental device, and then we present our results on characterization, showing how it becomes possible to observe each instability by inserting at the entrance of the column a diaphragm. Section 4 is devoted to the study of the transition to turbulence for the Kelvin-Helmholtz and centrifugal instabilities. We finally summarize our main results in conclusion.

2. LOW FREQUENCY INSTABILITIES : ELEMENTS OF THEORY

Drift waves are low frequency oscillations of the ionic and electronic populations of the plasma. They are driven by a pressure gradient transverse to the magnetic field. In a

cylindrical column, where there is a radial density gradient, their propagation is mainly azimuthal, but one important feature is that this propagation has also an axial component. A strong coupling between movement of the electrons along the magnetic field lines and ions in the transverse direction characterize their dynamics. Several mechanisms are known to destabilize drift waves, such as the existence of a radial electric field, axial current and collisions [5].

The centrifugal instability in plasmas is analogous to the Rayleigh-Taylor instability in hydrodynamics [6], which happens when a heavy fluid is supported against gravity by a light fluid. Any perturbation at the interface between both fluids triggers the instability which allows them to exchange their relative places. In curved geometries, as in mirror machines or tokamaks, magnetic field gradient or curvature are responsible of an effective gravity which allows the instability to develop. In cylindrical geometry, the plasma rotation induced by a radial electric field acts as an effective gravity as well, which can trigger the instability. The phase velocity of fluctuations is purely azimuthal and equal to the **E**x**B** drift velocity of the plasma rotation.

The Kelvin-Helmholtz instability is another hydrodynamic instability, which is driven by a velocity shear. In a cylindrical plasma, it can appear when the **E**x**B** rotation is non uniform. As for centrifugal instability, its propagation is purely azimuthal, so that it is also a flute instability. Its phase velocity is equal to 0.2 – 0.6 times the maximum **E**x**B** drift velocity of the plasma.

Main observable features for each instability are based on criteria derived by Jassby [7] and summarized in the table 2.1 below.

Parameter	Drift waves	Centrifugal	Kelvin-Helmholtz
Velocity	$\frac{v_{D,e}}{1+k_\perp^2\rho_s^2} \pm v_E$	v_E	0.2 – 0.6 v_E
$k_{//}$	~ 1/L	0	0
Location	Max ($\omega_{D,i}$)	Max (dn/ndr)	Max (shear)
Most unstable modes	No restriction	m = 1 or 2	$m > 2\pi r_0/L$
$Max\left(\frac{e\tilde{\phi}}{k_B T_e}\right)$	1	1	>> 1
$Max\left(\frac{e\tilde{\phi}/k_B T_e}{\tilde{n}/n}\right)$	≤ 1	≥ 1	>> 1
Local radial phase variation of the potential fluctuations	≤ 45°	40 – 90°	90 – 180°

Tab. 2.1 – Summary of criteria used for the characterization of the instabilities

3. OBSERVATION OF THE INSTABILITIES

3.1 EXPERIMENTAL SETUP

Experiments are performed in the linear section of the low-β magnetized double plasma device MIRABELLE [8] displayed in figure 3.1. The plasma is produced by a thermoionic discharge in one of the two source chambers. Confinement is ensured in the central section by 24 coils which create a uniform magnetic field whose strength can be varied up to 120 mT. To avoid filamentary plasma, compensation coils are installed on each source chamber, allowing null axial field in front of the cathodes. The base pressure inside the device is of the order of

10^{-5} torrs and the working pressure in argon is typically 1-2. 10^{-4} torrs. A high transparency grid is located at the entrance of the column. Its biasing influences the axial drift of the particles and the radial profiles of density and potential, allowing a dynamical control of the plasma regime. Discharge current, magnetic field strength, pressure, and biasing of an internal tube inside the central section determine the plasma regime as well. In order to study the effects of stronger radial gradients, a metallic diaphragm, acting as a limiter, can also be inserted at the entrance of the column.
Radial profiles of mean value quantities are obtained with a 3D movable biasable probe located inside the plasma column. When used with a fixed probe for phase reference, it allows for conditional sampling measurements across the full section of the plasma column. Spatiotemporal measurements are also realized using an azimuthal array of 32 probes at the fixed radius r = 7 cm. The azimuthal mode number *m* and azimuthal phase velocity can be easily deduced from these measurements. Finally, parallel wave number is determined using two parallel langmuir probes.

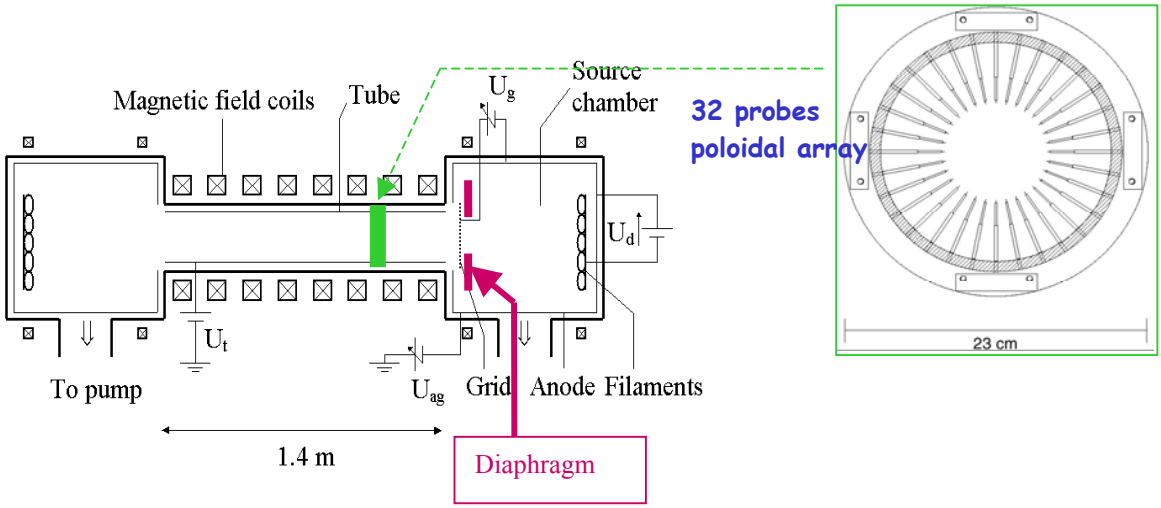

Fig. 3.1 – Schematic drawing of the MIRABELLE device

3.2 RESULTS WITHOUT LIMITER

Characterization mainly lies on very precise measurements of radial profiles of mean value quantities. Theoretical propagation velocity for each instability is computed from gradients of density, plasma potential and electronic temperature, as it can be seen in Fig. 3.2. Then it is compared to the phase velocity of the fluctuations deduced from conditional sampling measurement, or from autocorrelation of time series of the floating potential. Measurements are repeated for a large set of discharge parameters. The most remarkable evolution is observed when the magnetic field value is varied. The experiments are performed for values ranging from 20 to 110 mT. The **ExB** drift velocity is negligible whatever the magnetic field intensity, whereas the propagation velocity for drift waves is in very good agreement with the phase velocity of the fluctuations, as it can be seen in Fig. 3.3. A subsequent measurement leads to the conclusion that the parallel wavelength is long, of the order of twice the length of the plasma column, but not infinite. Moreover, analysis of the fluctuations reveals that the amplitude of density fluctuations is bigger than the one of potential fluctuations, and no noticeable radial variation of the phase of potential fluctuation is recorded.
Thus, without the limiter, we observe that instabilities are not affected by the very low radial equilibrium electric field, and only drift waves are excited in the plasma column.

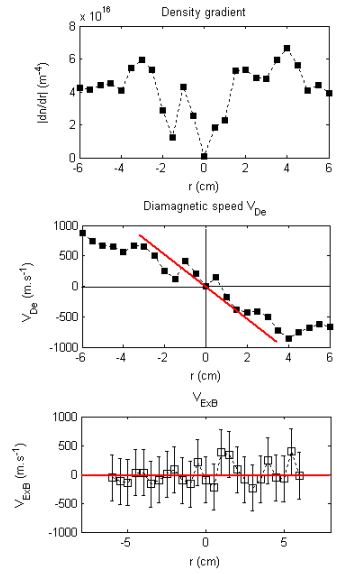

Fig. 3.2 – Profiles of density gradient, diamagnetic and **ExB** velocities, with B = 80 mT, without limiter.

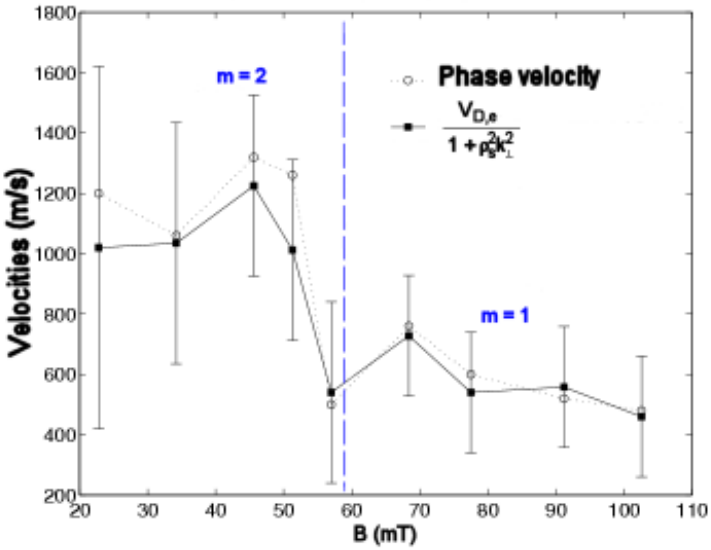

Fig. 3.3 – Phase velocity and propagation velocity for drift waves according to the magnetic field value, without diaphragm. One notice a very good agreement between both velocities.

3.3 RESULTS WITH LIMITER

Without any limiter, the diameter of the column is determined by the diameter of the tube, i.e. 24 cm. To study effect of stronger gradients, we introduce at the entrance of the column a metallic diaphragm of diameter 15 cm. According to the magnetic field magnitude, three different regimes, each corresponding to a different instability, can be observed.

When B > 70 mT, comparison between experimental data and Tab. 2.1 shows without any doubt that only drift waves are excited. As in the case without limiter, the radial equilibrium electric field is very low, and radial profiles are only determined by the magnitude of the magnetic field.
When B < 50 mT, strong radial equilibrium electric field are observed at the edge of the limiter. The resulting **ExB** drift is of the same order of magnitude as the theoretical propagation velocity for drift waves. At the radial location corresponding to the maximum level of fluctuations, the phase velocity of the fluctuations is about 0.6 to 0.7 times the **ExB** drift velocity. If these fluctuations were drift waves, the **ExB** rotation would add a Doppler shift to the phase velocity, so that the phase velocity should be greater. On the other hand, this result is in good agreement with flute modes, especially if the Kelvin-Helmholtz instability is considered. Moreover, both velocities are sheared, and conditional sampling reveals spiral structures (Fig. 3.4).
The hypothesis of flute modes is confirmed by measurements of the parallel wave number, whose mean value is zero. Variation of this parameter according to the magnitude of the B field clearly demonstrates that a transition between flute modes and drift waves occurs when B is increased (Fig. 3.5).
Finally, measuring the radial variation of the phase (Fig. 3.6) and the ratio between potential and density fluctuations (Fig. 3.7), it becomes clear that we have a Kelvin-Helmholtz instability.

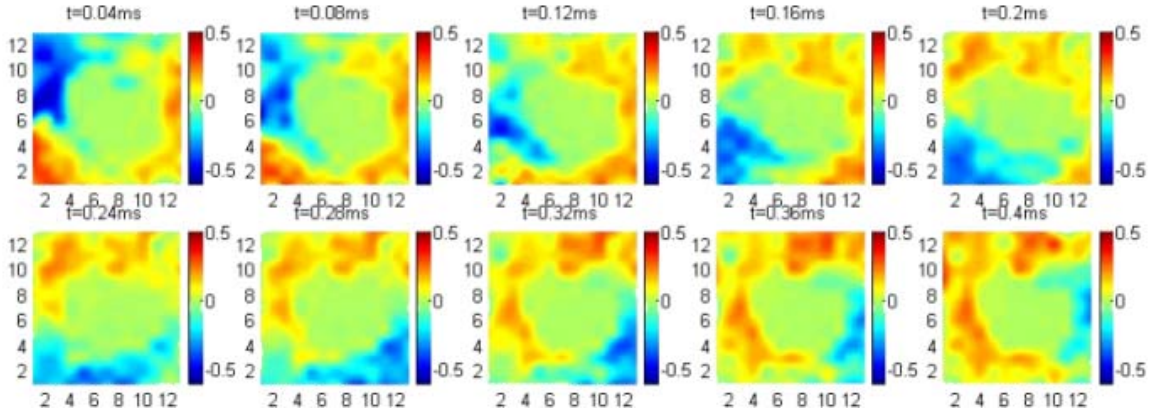

Fig. 3.4 – Azimuthal propagation of a spiral mode m = 1 for the density fluctuations, with the ∅ 15 cm limiter, B = 22 mT.

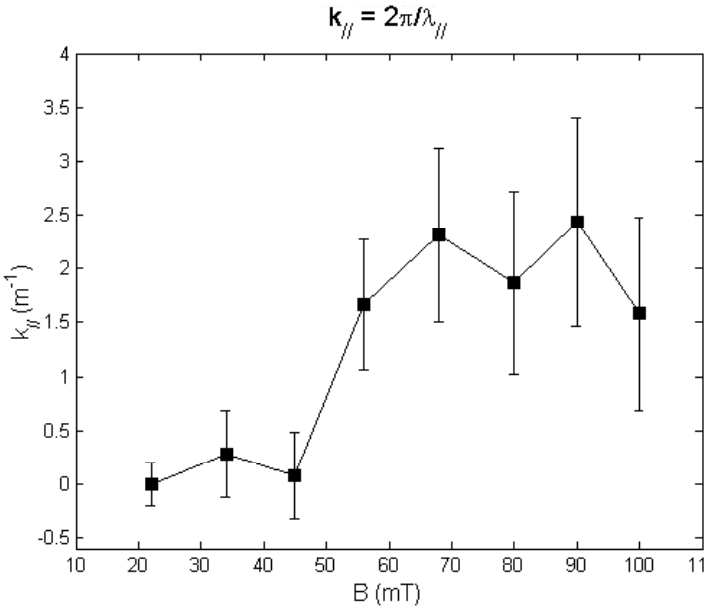

Fig. 3.5 – Evolution of the axial wave number according to the magnetic field magnitude, with the ∅ 15 cm limiter.

A transition between drift waves and the Kelvin-Helmholtz instability is then expected when B is in the range 50-70 mT. But investigations of regimes in this range don't show a clear transition from one regime to another. By adjusting other discharge parameters, it is possible to keep unstable modes with periodic fluctuations whose frequency slowly decreases when B is increased. In a first transition scenario, it is not possible to clearly distinguish between both instabilities because of experimental uncertainties. Either the system permanently slides between a regime dominated by the Kelvin-Helmholtz instability and another dominated by drift waves, or both instabilities coexist. According to the other discharge parameters, another transition scenario is however possible, where a centrifugal instability is observed. The phase velocity of the fluctuations is then equal to the **ExB** drift velocity and is far below the propagation velocity expected for drift waves. There is no axial phase shift, but a $\pi/2$ radial variation of the phase of the potential fluctuations is recorded. Amplitude of density and potential fluctuations are also in very good agreement with what is expected for a centrifugal instability (cf. Fig. 3.8 & 3.9).

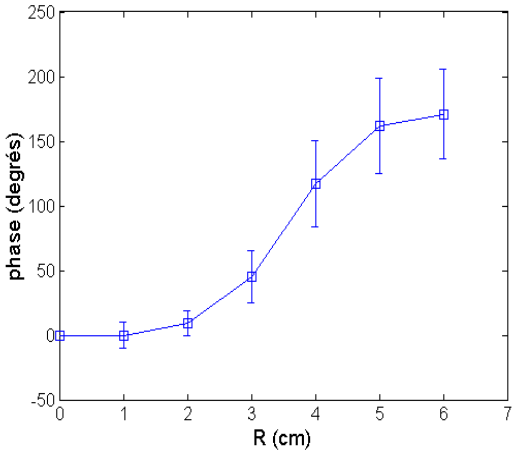

Fig. 3.6 – Radial variation of the phase of the potential fluctuations, with the ∅ 15 cm limiter, B = 22 mT.

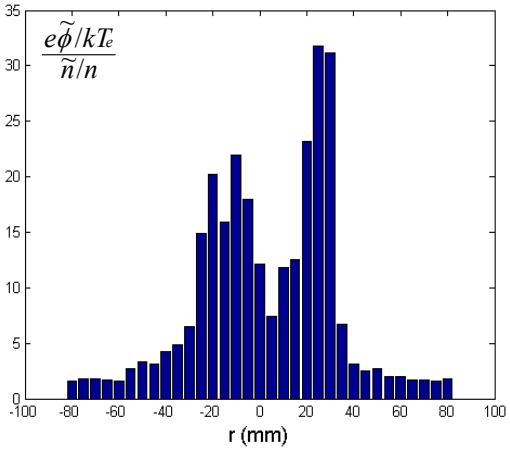

Fig. 3.7 – Ratio between potential and density fluctuations, with the ∅ 15 cm limiter, B = 22 mT.

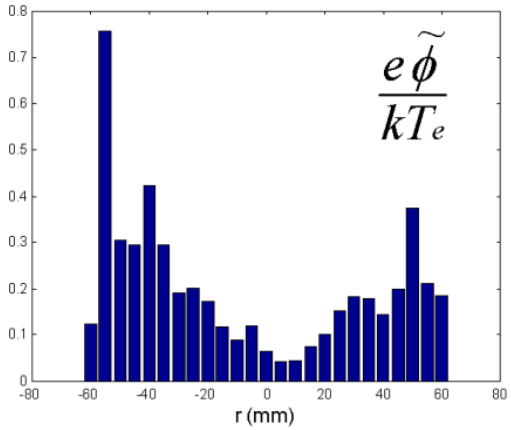

Fig. 3.8 – Amplitude of potential fluctuations, with the ∅ 15 cm limiter, B = 66 mT.

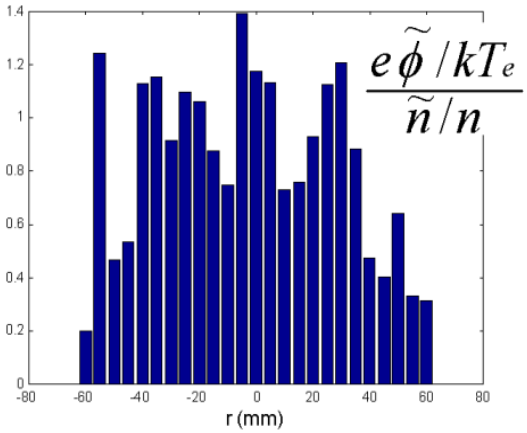

Fig. 3.9 – Ratio between potential and density fluctuations, with the ∅ 15 cm limiter, B = 66 mT.

When the diameter of the limiter is reduced to 10 cm, the same characterization leads to the conclusion that only the Kelvin-Helmholtz instability is observed in the range 10-110 mT. In particular, we note that all velocities are strongly sheared and that the theoretical propagation velocity for drift waves is far beyond the phase velocity of the fluctuations, which is very close to the **ExB** drift velocity (Fig. 3.10 & 3.11).

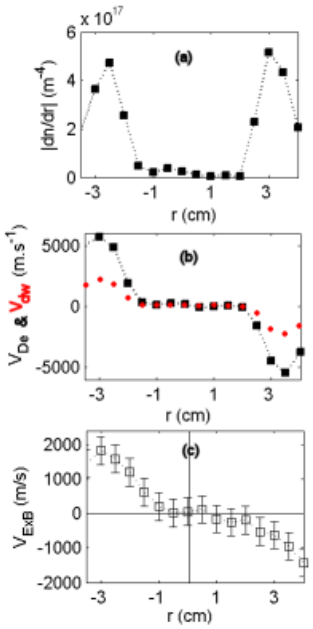

Fig. 3.10 – Profiles of density gradient, diamagnetic and **ExB** velocities, with B = 80 mT, with the ∅ 10 cm limiter.

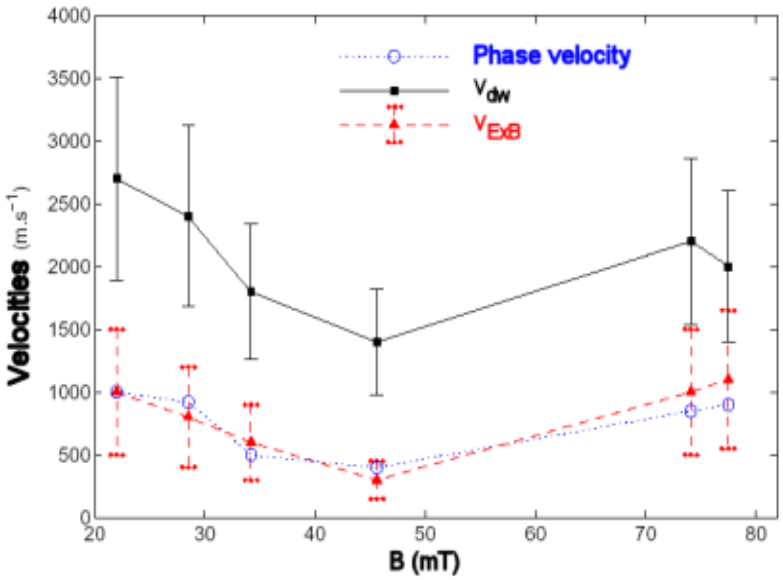

Fig. 3.11 – Phase velocity, **ExB** drift velocity and propagation velocity for drift waves according to the magnetic field value, with the ∅ 10 cm limiter.

3.4 TRANSITION BETWEEN INSTABILITIES

Depending on whether a diaphragm reduces or not the plasma diameter, and according to its diameter and the magnetic field intensity, we demonstrated that three instabilities can be observed in our device : drift waves, and rotational Kelvin-Helmholtz and centrifugal instabilities, as it is summarized in Fig. 3.12. Looking at the radial location of the fluctuations in the different cases, we obtain Fig. 3.13. This figure shows that drift waves are excited when the location of fluctuations, and thus profiles, only depend on the intensity of the magnetic field. When the intensity of the magnetic field doesn't play this role, as with the diaphragm of diameter 10 cm, the strong radial electric field at the edge of the limiter excites a Kelvin-Helmholtz instability.

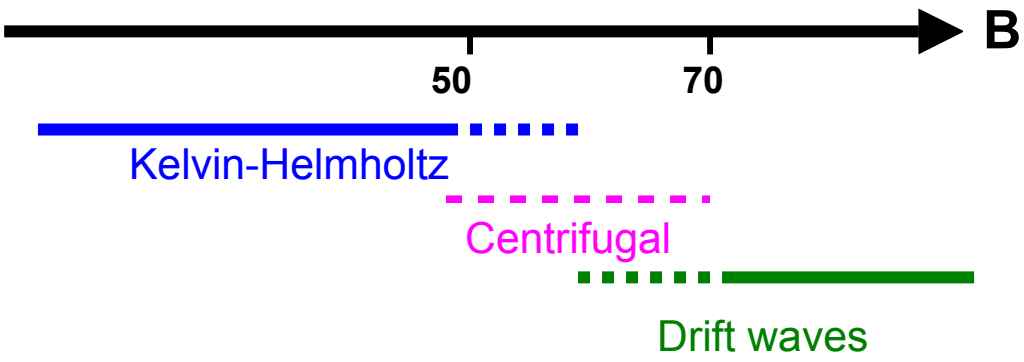

Fig. 3.12 – Observation of the instabilities with the ∅ 15 cm limiter

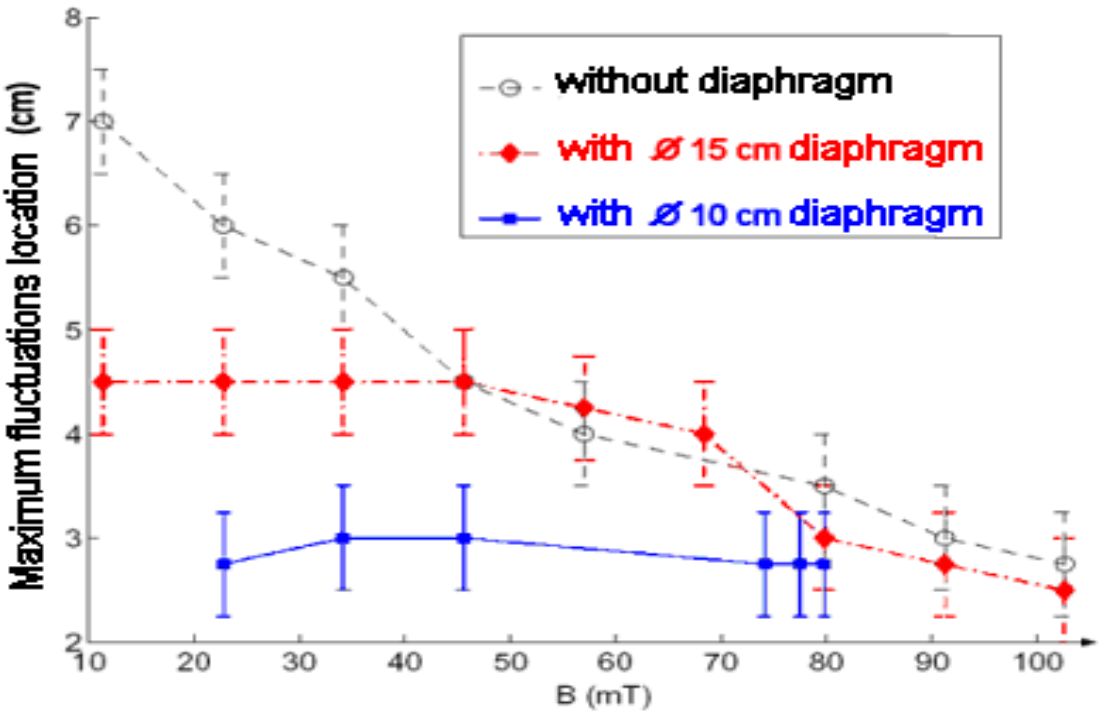

Fig. 3.13 – Radial location of the maximum of the floating potential fluctuations according to the magnetic field magnitude, with and without the two limiters.

The case of the diaphragm of diameter 15 cm is the most explicit. When the magnetic field is low (B < 50 mT), profiles are imposed by the limiter. The resulting **ExB** drift velocity is sheared in the radial direction, giving birth to a Kelvin-Helmholtz instability. When the magnetic field is high (B > 75 mT), the reference length scale ρ_s is smaller than the length scale due to the diaphragm L_D, whose influence is no more perceptible. In between, ρ_s and L_D are very close. The effect of the limiter declines without disappearing, and a centrifugal instability can be observed.

4. TRANSITION TO TURBULENCE

4.1 TRANSITION OF DRIFT WAVES

For a few years, drift waves are known to follow the Ruelle-Takens-Newhouse route to turbulence, in which chaos and turbulence are a consequence of the non linear interaction between two modes with incommensurable frequencies [9]. The control parameter used in this experiment was the biasing between the tube and the ground. This parameter allows to modify the **ExB** rotation, what is a well known mean of destabilization for drift waves [10]. Using a poloidal array of probes, it was shown that drift waves transition to turbulence to chaos and turbulence is a spatio-temporal phenomenon. Thus, spatio-temporal control experiments based on control chaos techniques showed a better efficiency in controlling weakly turbulent drift waves regimes than purely temporal methods [11-12].
In our work, we recovered the RTN route and we used recent analysis tools to study the quasi-periodic and chaotic regimes : the Morlet wavelet transform and the empirical mode decomposition [13-14]. Both techniques are used to analyse non stationary signals and allow reconstruction of the time/frequency evolution of the signal. Using them, we demonstrated

that regimes looking like chaotic when analysed with a classical Fourier transform keep in fact a high degree of temporal organization. This point is illustrated by Fig. 4.1 & 4.2.

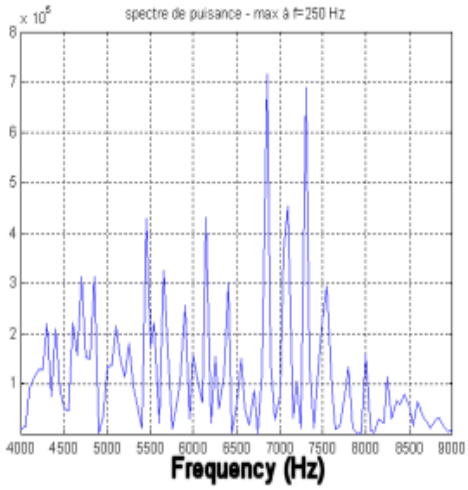

Fig. 4.1 – Fourier spectrum showing great similarity with a chaotic regime.

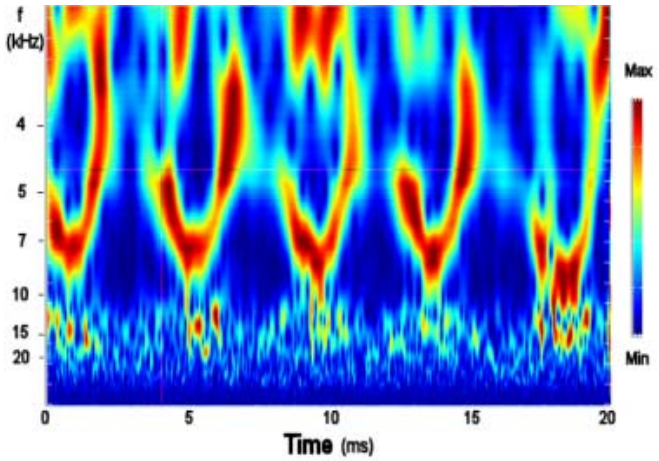

Fig. 4.2 – Morlet wavelet analysis of the signal whose Fourier spectrum is figured on the left. Time evolution of the frequency shows evidence of periodicity.

4.2 TRANSITION OF A KELVIN-HELMHOLTZ INSTABILITY

Observation of the Kelvin-Helmholtz instability in our device requires a limiter. By reducing the plasma diameter, it doesn't allow for using the tube polarization as a control parameter anymore, since there is no more plasma close enough to the tube. To study the Kelvin-Helmholtz transition to turbulence, we thus used the discharge voltage (relative biasing of the anode to the cathode) as a new control parameter.

Measurements in the velocity shear layer show that the Kelvin-Helmholtz instability follows the Ruelle-Takens-Newhouse transition scenario as well. This is illustrated in Fig. 4.3, where we can see the transition from a periodic m = 1 mode of frequency F_1 = 6 kHz (a-d) to a quasi-periodic regime with two incommensurable frequencies F_1 = 6 kHz and F_2 = 11.8 kHz (e-h). Varying again the control parameter then leads to a turbulent regime (Fig. 4.3 (i-l)).

Moreover, measurements with the 32 poloidal probe array and with the 3D movable probe at different radial positions clearly indicate that the transition to chaos and turbulence is a spatio-temporal phenomenon. As an example, Fig. 4.4 and 4.5 show the transition from an azimuthal m = 1 mode to a regime where both m = 1 and m = 2 modes exist simultaneously. If the control parameter is still increased, other modes appear and coexist, making the system more and more complex (Fig. 4.6). Moreover, comparison between radial variation of the frequency and the mode structure shown at r = 7 cm by the 32 probe array gives clear evidence that azimuthal mode number *m* have a radial distribution very close to the one of drift waves : with increasing mode number, position of maximum density fluctuation shifts radially outwards.

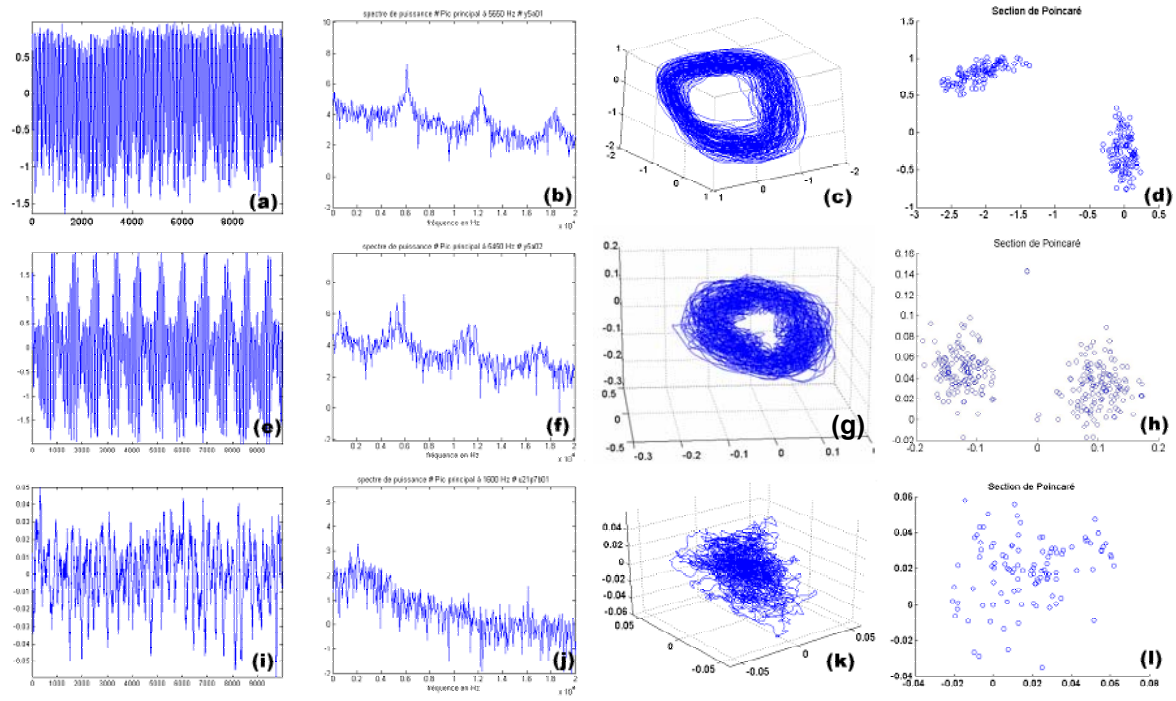

Fig. 4.3 – Temporal transition to turbulence of the Kelvin-Helmholtz instability. From left to right, signal, Fourier spectrum, phase portrait and its Poincaré section for the periodic (a-d), the quasi-periodic (e-h), and the turbulent regimes (i-l).

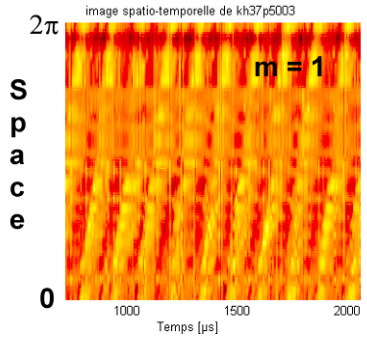

Fig. 4.4 – Spatio-temporal image of a regular m = 1 mode (U_{ac} = 37.5 V).

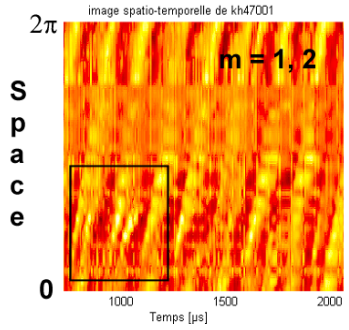

Fig. 4.5 – Spatio-temporal image showing bifurcation from a m = 1 to a m = 2 mode (U_{ac} = 47 V).

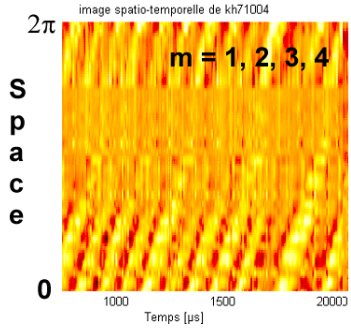

Fig. 4.6 – Spatio-temporal image showing m = 1, 2, 3 and 4 (U_{ac} = 71 V).

Wavelet analysis of the quasi-periodic regime corresponding to Fig. 4.3 (e)-(h) exhibits a behaviour known as periodic pulling [15]. In Fig. 4.7, we see that the frequency periodically slides between two values. This can be interpreted as the incomplete synchronization of the m = 1 mode by the m = 2 mode. The reason why synchronization is not complete is probably that the coupling between driving and driven waves is too weak, or the frequency mismatch too large to establish complete synchronization. Thus, the reason why periodic pulling is only observed within the velocity shear layer is probably linked to the radial location of poloidal mode number described above.

Although we found that the RTN route to turbulence also exists for the Kelvin-Helmholtz instability, it is not the only scenario which allows the Kelvin-Helmholtz instability to evolve into a turbulent state. Another kind of transition can also be observed, where a weakly turbulent regime is the consequence of intermittency between two regimes, possibly quasi-

periodic. Fig. 4.8 shows such a regime : spatio-temporal structure of the left side corresponds to a quasi-periodic regime with m = 1 and m = 2, whereas m = 3 and m = 4 cans be seen on the right side. This behaviour is also obvious in Fig. 4.9 showing time/frequency analysis of a temporal series recorded at r = 5 cm for the same regime.

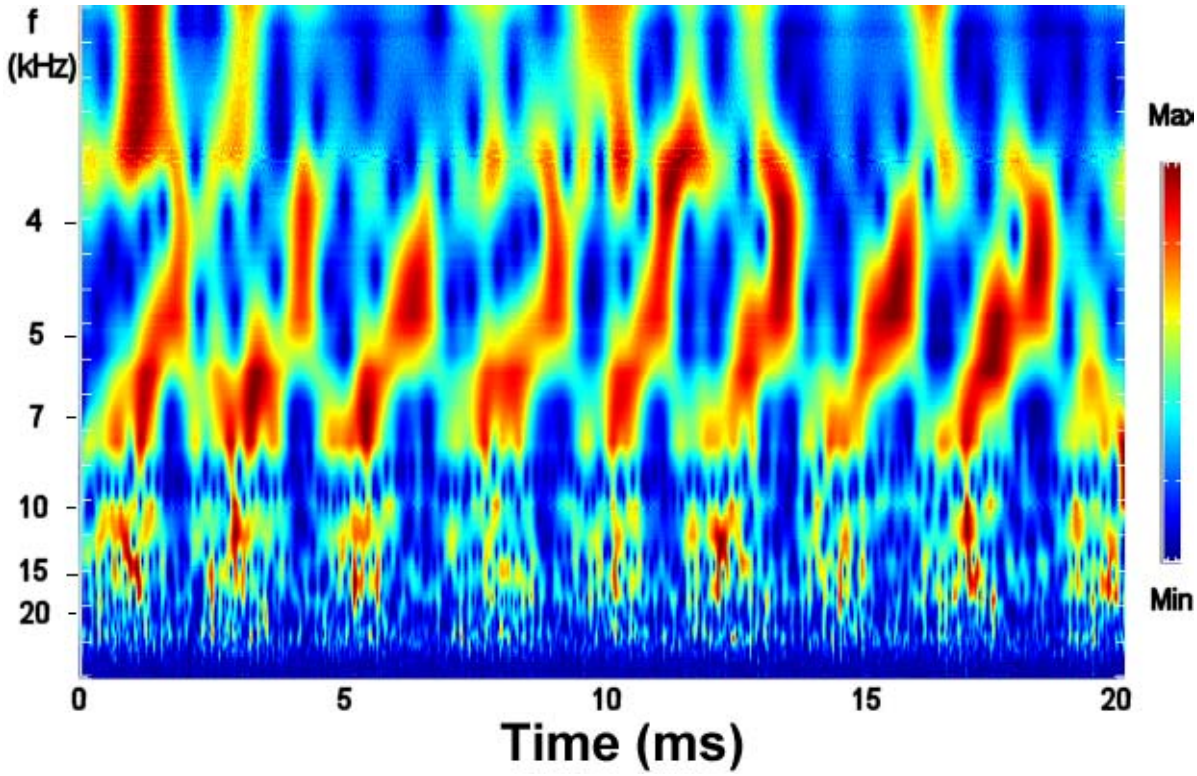

Fig. 4.7 – Morlet wavelet analysis of signal depicted in Fig. 4.3 (e-h). Time evolution of the frequency shows evidence of periodic pulling.

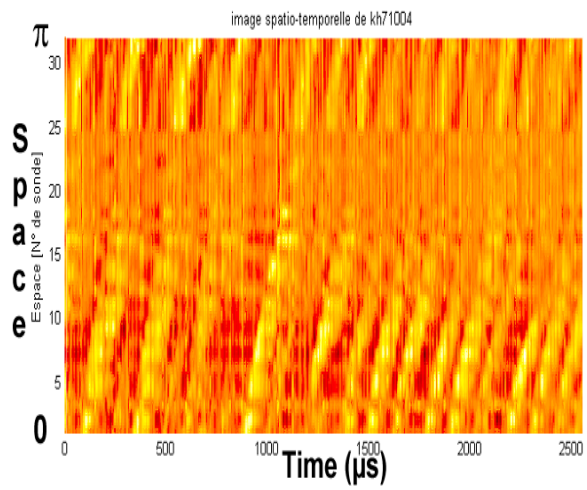

Fig. 4.8 – Spatio-temporal image showing intermittency between m = 1-2 (left) and m = 3-4 (right) (U_{ac} = 71 V).

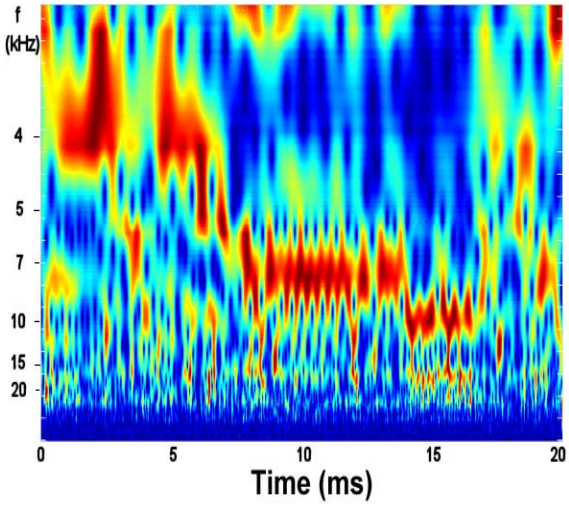

Fig. 4.9 – Morlet wavelet analysis of signal corresponding to the regime depicted in Fig. 4.8. Time evolution of the frequency shows intermittency.

4.3 TRANSITION OF A CENTRIFUGAL INSTABILITY

To observe the transition to turbulence of the centrifugal instability, we still use the discharge voltage as a control parameter. Once again, the RTN route is found to cause the transition,

chaos and turbulence being observed after a quasi-periodic regime involving m = 1 and m = 2 modes. As for the Kelvin-Helmholtz instability, temporal periodic pulling is observed in the quasi-periodic regime when both modes have appropriate amplitudes. However, analysis of the quasi-periodic regime indicate that frequency of the m = 2 mode is slighty lower than frequency of the first harmonic of the m = 1 mode (Fig. 4.10 & 4.11). Thus, dispersion relation of the centrifugal instability is expected to have a different behaviour than the drift waves and Kelvin-Helmholtz ones.
Finally, simultaneous measurements at two different radial positions show that transition to turbulence first appears near to the maximum of the density gradient, and then in the outer part of the plasma column when the control parameter is varied. This gives clear evidence that transition to turbulence of the centrifugal instability is a spatio-temporal phenomenon, as for drift waves and Kelvin-Helmholtz instabilities.

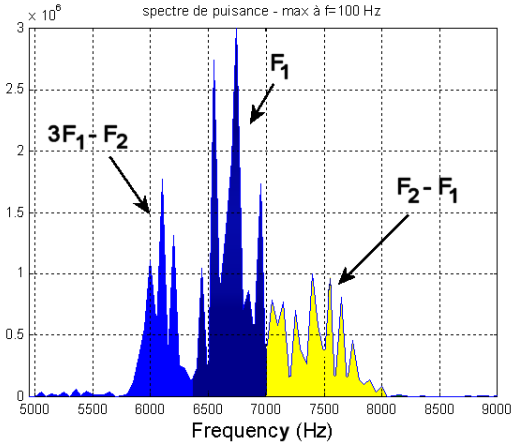

Fig. 4.10 – Fourier spectrum of the quasi-periodic regime showing non linear interactions between m = 1 and m = 2 modes, during transition to turbulence of a centrifugal instability.

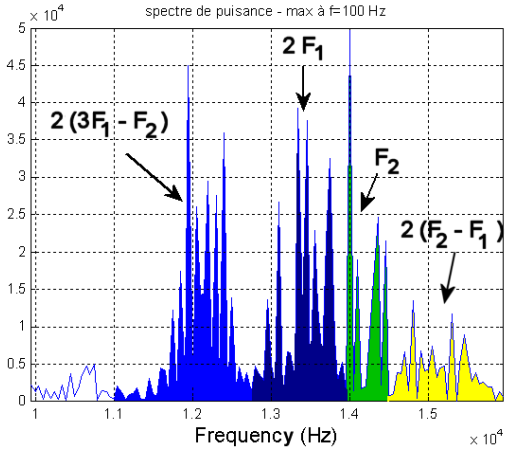

Fig. 4.10 – Fourier spectrum of the quasi-periodic regime showing non linear interactions between m = 1 and m = 2 modes (harmonics).

5. CONCLUSION

We reported on the observation of three kinds of low frequency instabilities and their transition to turbulence in a low-β magnetized plasma column. In the general case where radial profiles only depend on the magnetic field strength, density fluctuations are identified as being drift waves. However, restriction of the plasma diameter by a limiter allows for observation of Kelvin-Helmholtz and centrifugal instabilities as well, according to the magnetic field strength and diameter of the limiter. When ρ_s is large enough compared to the length scale due to the limiter, a Kelvin-Helmholtz instability due to the shear of the **ExB** velocity is observed. On the other hand, when ρ_s is is smaller than the length scale due to the limiter, profiles only depend on the magnetic field strength : **ExB** velocity is very low, and only drift waves are recorded. Finally, in between, centrifugal instability excited by homogeneous **ExB** rotation can be observed.
We then demonstrated that a similar transition to turbulence exists for each instability. In this scenario, known as Ruelle-Takens-Newhouse route, a quasi-periodic regime evolves to chaos and turbulence consecutively to nonlinear interactions between two modes of incommensurable frequencies. Moreover, we demonstrated in the three cases that this transition was a spatio-temporal phenomenon. However, in the case of the Kelvin-Helmholtz

instability, another scenario was also found in which turbulence arises from intermittency between two regimes, possibly quasi-periodic themself.
Next step of this work will consist in applying to Kelvin-Helmholtz and centrifugal instabilities control methods which have already proved their efficiency on drift waves.

BIBLIOGRAPHY

[1] E. Gravier *et al*., *Physics of Plasmas*, **11** (2004) 529-537.
[2] T. Klinger *et al*., *Phys. Rev. Let.*, **79**, 20 (1997).
[3] N. D'Angelo and R.W. Motley, *Phys. Fluids*, **6**, 422 (1963)
[4] W. Horton, *Rev. Modern Physics*, **71** (3), 735 (1999)
[5] C. Schröder, PhD thesis, Ernst-Moritz-Arndt University, Greifswald, 2003.
[6] S. Chandrasekhar, Hydrodynamic and hydromagnetic stability, Oxford University Press, London, 1961, Ch. XI.
[7] D.L. Jassby, *Phys. Fluids*, 15 (9), 1972.
[8] T. Pierre, G. Leclert, F. Braun, *Rev. Sci. Instrum*. 58, (6), 1987.
[9] T. Klinger *et al*., *Phys. Rev. Lett*., 79, 1997, 3913-3916.
[10] E. Marden-Marshall, PhD thesis, Darmouth College, Hanover, New Hampshire, 1980.
[11] E. Gravier *et al*., *Phys. Plasmas*, 6 (5), 1999, 1670-1673.
[12] T. Klinger *et al*., *Phys. Plasmas*, 8 (5), 2001, 1961-1968.
[13] P. Gaillot, PhD thesis, Université de Toulouse III, 2000.
[14] N.E. Huang et al., *Proc. Roy. Soc. London A*, Vol. 454, 1998, 903-995.
[15] M.E. Koepke, T. Klinger, F. Seddighi, A. Piel, *Phys. Plasmas,* 3 (12), 1996.